

# MICROFLUIDIC MEASUREMENTS OF DIFFUSION COEFFICIENTS OF $ZnCl_2$ -DMSO ELECTROLYTES FOR ZN-ION BATTERIES

Binbin Chen<sup>1</sup>, Jin Xuan<sup>2</sup>, Gregory James Offer<sup>1</sup>, Huizhi Wang<sup>1\*</sup>

<sup>1</sup>Department of Mechanical Engineering, Imperial College London, UK

<sup>2</sup>Department of Chemical Engineering, Loughborough University, Loughborough, UK

\*Corresponding author. huizhi.wang@imperial.ac.uk (HW)

## ABSTRACT

Ion diffusivity is one of the most important properties in the electrolyte for batteries, as poor mass transport can cause large performance losses during operation. Therefore, the understanding of the relations between diffusivity and electrolyte conditions, such as compositions and concentrations, is crucial for designing proper electrolytes for batteries. In this paper, we investigate the diffusion of zinc ions in  $ZnCl_2$ -DMSO electrolytes using microfluidics with fluorescence microscopy. It is found that the diffusion of zinc ions in the electrolytes is sensitive to concentration variations.

**Keywords:** Diffusivity, Zinc-ion battery, Microfluidics, Fluorescence microscopy

## NONMENCLATURE

### Abbreviations

PMMA	Poly(methyl methacrylate)
DMSO	Dimethyl sulfoxide
$ZnCl_2$	Zinc chloride

### Symbols

Re	Reynolds number
z	Distance downstream the channel
v	Average flow rate
H	Thickness of the channel
D	Diffusion coefficient
$\delta$	Diffusion broadening width

## 1. INTRODUCTION

Zinc-ion battery normally consists of a zinc anode and a zinc-ion intercalating cathode in a zinc-salt

electrolyte and uses zinc ions as charge carriers during operation.[1] The electrolyte transporting zinc ions between the anode and the cathode plays an essential role in determining battery performance and life. Understanding of the ion transport properties in the electrolytes can give insights into electrolyte dynamics as well as battery processes.[2] Yet, the transport of ions in electrolytes is generally complex, especially in organic electrolytes, which usually requires lots of efforts to study.[3] So far, the zinc ion diffusion characteristics have not been studied in organic electrolytes. DMSO, which is chemically stable and has relatively high permittivity, has been treated as a good solvent candidate for electrolytes as it has the ability to stabilize the electrolyte from water decomposition and is beneficial for maintaining  $Zn/Zn^{2+}$  redox reversibility and cyclability.[4]

In this study, we investigate the zinc ion transport in  $ZnCl_2$ -DMSO electrolytes using a microfluidics-based fluorescence microscopy platform. The concentration dependency of the diffusion properties is analyzed. In the micro-channel, liquids rely on conditions of low Reynolds numbers ( $Re$ ) to form laminar flow.[5] Fluids with different compositions enter separate inlets and merge to flow adjacently, in which no mechanical mixing of streams occurs and the concentration distribution changes only by diffusion of compositions across the interfaces.[6] Fluorescent sensors, with high sensitivity of fluorescence assays,[7] is used to visualise the diffusion of zinc ions in the channel. The developed platform is demonstrated to be a cheaper and easier-to-access tool for diffusion characterisation. The microfluidic tool is generally applicable to other electrolytes apart from the  $ZnCl_2$ -DMSO electrolytes, which can be useful for guiding future electrolyte development and battery performance improvement.

Selection and peer-review under responsibility of the scientific committee of the 11th Int. Conf. on Applied Energy (ICAE2019).

Copyright © 2019 ICAE

## 2. METHODOLOGY

### 2.1 Chemicals

Chemicals of  $\text{ZnCl}_2$  (99.9%) and DMSO (99.7%) were purchased from VWR and used as electrolyte salt and solvent. DMSO-based  $\text{ZnCl}_2$  electrolytes with different concentrations, from 0.1 mM to 100 mM, were prepared by dissolving  $\text{ZnCl}_2$  powder in DMSO.

Zinc-ion fluorescent probe (Zinquin ethyl ester,  $\text{C}_{21}\text{H}_{22}\text{N}_2\text{O}_5\text{S}$ , excitation 368nm and emission 490nm) is commercially available from Enzo Life Science.  $\text{C}_{21}\text{H}_{22}\text{N}_2\text{O}_5\text{S}$  was used as zinc-ion indicator by dissolved in  $\text{ZnCl}_2$  DMSO-based electrolytes as sample solutions. A blank solution with the same concentration of probe was prepared by dissolving the  $\text{C}_{21}\text{H}_{22}\text{N}_2\text{O}_5\text{S}$  in DMSO.

### 2.2 Cell design and fabrication

Figure 1 shows the schematic illustration of the setup for ion diffusivity investigation, including micro-syringe pump, fluorescent microscope with PC and a Y-shape microfluidic platform. The Y-shape channel structure consists of three poly(methyl methacrylate) (PMMA) layers cut out by a carbon dioxide laser ablation system (VLS 2.30, Universal Laser System, USA). The top layer seals the assembly with two inlets and an outlet for fluidic electrolyte access. The two inlets connect with the sub-branches of the Y-shape channel in the middle layer, respectively. The dimensions of the junction channel are 0.5 mm  $\times$  3.3 mm  $\times$  16 mm (thickness  $\times$  width  $\times$  length). The slit-like channel with high aspect ratio of width and thickness ensures a same velocity profile across the major of width range.

The sample and blank solutions were pumped into the cell by a syringe pump (LSP02-1B, LongerPump, China) at flow rates ranging from 50  $\mu\text{l}/\text{min}$  to 300  $\mu\text{l}/\text{min}$ , corresponding to low enough Reynolds number from 0.28 to 1.66, which ensures laminar flow pattern in the channel.[8] With a concentration difference of zinc ion between two solutions, diffusion of zinc ion occurs when two solutions flow adjacently.



**Figure 1** Experimental setup for ion diffusion measurements.

### 2.3 Fluorescent characterization

Visualisation of the ion diffusion was performed using the fluorescent microscope system (205FAC, Leica, UK) with a DAPI filter. When the flow patterns within the microfluidic channel became stable, fluorescent images were captured. The exposure time was 30 seconds with a fluorescent intensity range of 0-2500 units. Intensity quantification was conducted at the downstream position of 10 mm from the junction point (green dash lines in Figure 3 & 5).

## 3. RESULTS

### 3.1 Emission intensity vs. concentration of zinc ion

To verify the 'turn-on' fluorescence instinct of  $\text{C}_{21}\text{H}_{22}\text{N}_2\text{O}_5\text{S}$  upon the addition of zinc ions, same volume of DMSO-based electrolytes with various concentrations of  $\text{ZnCl}_2$  were added into probe solutions with concentration of 15 mM  $\text{C}_{21}\text{H}_{22}\text{N}_2\text{O}_5\text{S}$  and observed with the fluorescent microscope. As shown in Figure 2, the intensity of emission is increased in a zinc ion concentration-dependent way till the concentration of zinc ion is comparable with that of probe, which suggested a 1:1 binding stoichiometry between the probe and zinc ion. This intrinsic binding ratio enables the detection of the concentration profile of zinc ion with the fluorescent intensity with the channel.

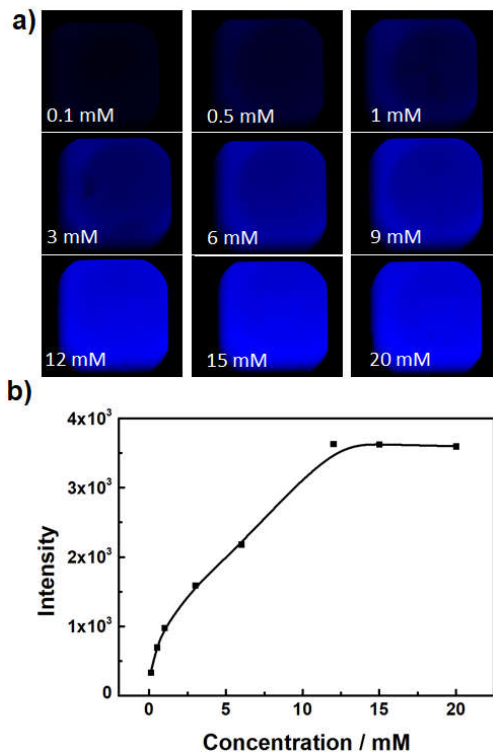


**Figure 2** a) Fluorescent images of emission and b) change of emission intensity of 15 mM zinc ion probe solution with the addition of ZnCl<sub>2</sub> electrolyte with increasing concentration (0.1 mM – 20 mM).

### 3.2 Interfacial mixing under different flow rates

Figure 3 shows the fluorescent images of the illuminated channel obtained by injecting sample solution with 100 mM ZnCl<sub>2</sub> showing zinc ion diffusion at different flow rates. The bright and dark areas on the bottom and top sides correspond to solutions with/without zinc ions. Four trials were conducted at flow rates of 300 μl/min, 200 μl/min, 100 μl/min and 50 μl/min. The effect of decreasing the flow rate is to increase the average residence time and thereby increase the extent of interdiffusion of zinc ion from sample solution to blank solution. At high flow rate, a trenchant interface between the two streams is observed. While at low flow rates, concentration gradient zone due to ion diffusion is clearly observed.

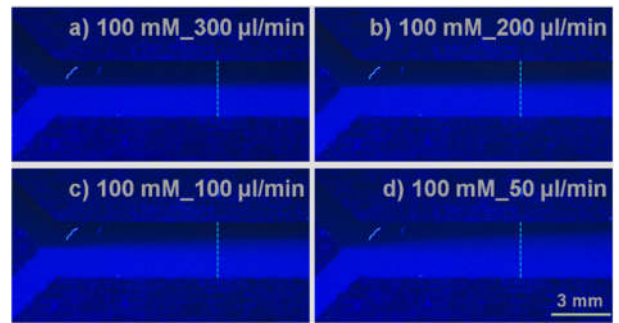


**Figure 3** Fluorescent images of the illuminated channel at different flow rates showing zinc ion diffusion (Sample solution: 100 mM ZnCl<sub>2</sub> + C<sub>21</sub>H<sub>22</sub>N<sub>2</sub>O<sub>5</sub>S + DMSO; Blank solution: C<sub>21</sub>H<sub>22</sub>N<sub>2</sub>O<sub>5</sub>S + DMSO).

The fluorescent intensities at z=10 mm position in the channel in Figure 3 under different flow rate were measured, shown in Figure 4 (a). To aid in quantifying the diffusion constant, a smooth fitting with method of ‘adjacent-average’ was performed with ORIGIN to smooth the intensity profile. The diffusion width ( $\delta$ ) can be obtained from the cross-section intensity profile in Figure 4 (a). Figure 4 (b) shows the plot of three power of diffusion width ( $\delta$ ) versus the average contacting time ( $z/v$ ) and channel thickness ( $H$ ), which matches the scaling laws proposed by Ismagilov et al.,[9]

$$\delta^3(z, v) \sim \frac{DH^2}{v} \quad (1)$$

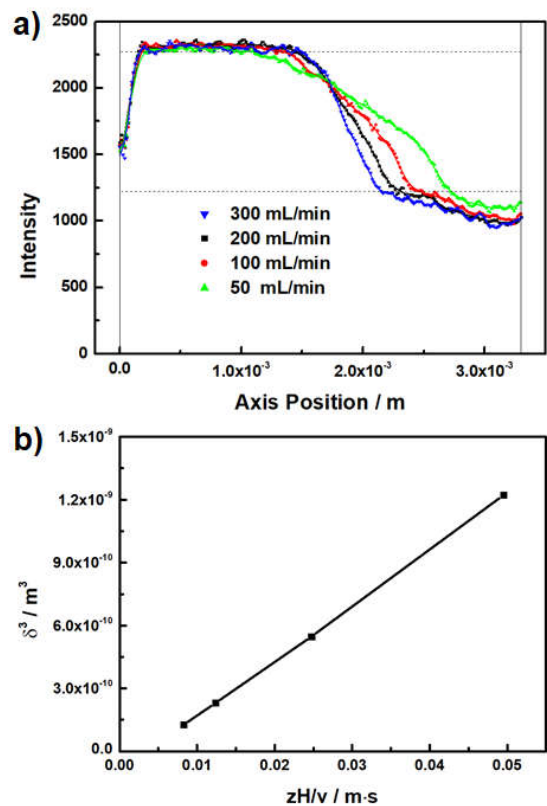


**Figure 4** a) Intensity profile of fluorescent emission across the sectional positions shown in Figure 3. b) Linear dependence

of three power of diffusion width ( $\delta^3$ ) vs. average contacting time and the thickness of the channel.

### 3.3 Concentration-dependent diffusion of zinc ions

Figure 5 shows the comparison of diffusion of sample solution with different concentrations of  $\text{ZnCl}_2$  at the flow rate of  $50 \mu\text{l}/\text{min}$ . A clear reduce in the diffusion zone can be observe when concentration decreases from  $100 \text{ mM}$  to  $0.1 \text{ mM}$ , corresponding to a decrease of diffusivity. Under reasonable assumptions, the concentration distribution fits a Gaussian profile [10]:

$$C(x) = \frac{Q}{\sqrt{4\pi Dt}} \exp\left(-\frac{x^2}{4Dt}\right) \quad (2)$$

where  $x$  is the axial distance,  $D$  is the diffusion coefficient, and  $t$  is the average residential time. The magnification of the diffusion coefficient of zinc ion in the solution with lower concentration is calculated around  $10^{-10} \text{ m}^2/\text{s}$ , which is comparable with the results determined by Taraszewska et al. in slightly different conditions.[11] When the concentration increase to  $100 \text{ mM}$ , the magnification of diffusion coefficient increase to  $10^{-9} \text{ m}^2/\text{s}$ , which indicates that electrolyte with higher concentration of  $\text{ZnCl}_2$  provides better transport properties.

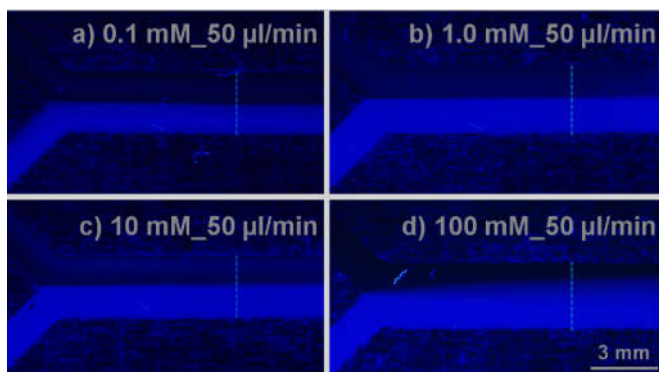


**Figure 5** Fluorescent images of the illuminated channel at  $50 \mu\text{l}/\text{min}$  showing zinc ion diffusion in solutions with different concentrations (Sample solution:  $0.1 \text{ mM} - 0.1 \text{ M ZnCl}_2 + \text{C}_{21}\text{H}_{22}\text{N}_2\text{O}_5\text{S} + \text{DMSO}$ ; Blank solution:  $\text{C}_{21}\text{H}_{22}\text{N}_2\text{O}_5\text{S} + \text{DMSO}$ ).

## 4. CONCLUSIONS

In summary, we demonstrated a microfluidic-based fluorescence microscopy platform for characterising zinc ion transport in the DMSO-based electrolytes for zinc ion batteries. With a zinc ion indicator ( $\text{C}_{21}\text{H}_{22}\text{N}_2\text{O}_5\text{S}$ ) yielding fluorescent signal, the diffusion of zinc ion in DMSO-based electrolytes was directly visualised. The linear relation of three power of diffusion width with flow rates was verified.

Furthermore, the diffusion of zinc ion in  $\text{ZnCl}_2$ -DMSO electrolyte was found highly dependent on electrolyte concentration.

## ACKNOWLEDGEMENT

The research is supported by the UK Engineering and Physical Sciences Research Council (EPSRC) via grant number EP/S000933/1.

## REFERENCE

1. Kundu, D., et al., *A high-capacity and long-life aqueous rechargeable zinc battery using a metal oxide intercalation cathode*. Nature Energy, 2016. **1**(10): p. 16119.
2. Han, S.-D., et al., *Origin of electrochemical, structural, and transport properties in nonaqueous zinc electrolytes*. ACS applied materials & interfaces, 2016. **8**(5): p. 3021-3031.
3. Wang, H. and F. Wang, *In situ, operando measurements of rechargeable batteries*. Current Opinion in Chemical Engineering, 2016. **13**: p. 170-178.
4. Xu, M., et al., *Improved Zn/Zn (II) redox kinetics, reversibility and cyclability in 1-ethyl-3-methylimidazolium dicyanamide with water and dimethyl sulfoxide added*. Journal of Power Sources, 2014. **252**: p. 327-332.
5. Suh, Y.K. and S. Kang, *A review on mixing in microfluidics*. Micromachines, 2010. **1**(3): p. 82-111.
6. Kamholz, A.E. and P. Yager, *Theoretical analysis of molecular diffusion in pressure-driven laminar flow in microfluidic channels*. Biophysical journal, 2001. **80**(1): p. 155-160.
7. Jeong, Y. and J. Yoon, *Recent progress on fluorescent chemosensors for metal ions*. Inorganica Chimica Acta, 2012. **381**: p. 2-14.
8. Kamholz, A.E., et al., *Quantitative analysis of molecular interaction in a microfluidic channel: the T-sensor*. Analytical chemistry, 1999. **71**(23): p. 5340-5347.
9. Ismagilov, R.F., et al., *Experimental and theoretical scaling laws for transverse diffusive broadening in two-phase laminar flows in microchannels*. Applied Physics Letters, 2000. **76**(17): p. 2376-2378.
10. Miyamoto, K.-i., et al., *Chemical imaging of the concentration profile of ion diffusion in a microfluidic channel*. Sensors and Actuators B: Chemical, 2013. **189**: p. 240-245.
11. Taraszewska, J. and A. Wałęga, *A kinetic study of the  $\text{Zn}^{2+}/\text{Zn}$  (Hg) system in dimethylsulfoxide and water+ dimethylsulfoxide mixtures at various concentrations of  $\text{NaClO}_4$* . Journal of electroanalytical chemistry and interfacial electrochemistry, 1985. **185**(1): p. 3-13.